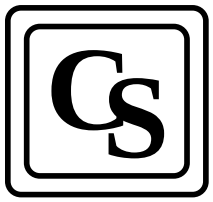

COMPUTER SCIENCE TECHNICAL REPORT

A Spectral Method for Solving Aerosol Dynamics

Adrian Sandu

CSTR-01-04
September 2001

Michigan Technological University, Houghton, MI 49931

A Spectral Method for Solving Aerosol Dynamics

Adrian Sandu*

*Department of Computer Science, Michigan Technological University, Houghton, MI 49931.

Abstract

This paper presents a discretization of particle dynamics equation based on spectral polynomial interpolation of the solution. Numerical tests show that the method achieves spectral accuracy in linear coordinates, and is able to reproduce well the reference solutions in logarithmic coordinates.
Keywords: Aerosol dynamics, spectral interpolation.

1 Introduction

As our understanding expands, new processes are incorporated into air quality computer models. One example is the particulate matter (aerosol) processes, the importance of which is now widely recognized. Aerosols are now a priority focus area in environmental science due to the leading role they play as a cause of adverse human health, and their ability to scatter and absorb incoming solar radiation and thus modify warming due to greenhouse gases and reduce visibility. Particulate matter (aerosol) processes are "emerging as a new frontier" in environmental studies (Nobel laureate P. Crutzen et. al. [4]).

To accurately study the effects of aerosols it is necessary to resolve aerosol number and mass distributions as a function of chemical composition and size. Treatment of aerosol processes leads to (at least) an order of magnitude increase in the overall computational time of an air quality model; this is mainly due to repeatedly solving the aerosol chemistry (or chemical equilibria) for different particle sizes. Therefore there is a clear need for rigorous, reliable and efficient computational techniques for aerosol simulations. In particular, there is a need for methods that accurately solve aerosol dynamics using a small number of size bins (discretization points), such that the time for aerosol chemistry calculations (which is proportional to the number of bins) is manageable.

In this paper we develop a method for solving the aerosol dynamics equations based on a semi-discretization in particle size followed by the time-stepping method of choice. The semi-discretization in size is based on a spectral polynomial interpolation of the solution. We also propose a second order linearly-implicit time stepping method. The presentation of the method is done in the context of single component particle populations described by number densities. The method can be directly extended to mass or volume densities and multiple component particles, as shown in Section 5.7.

The paper is organized as follows. Section 2 presents the particle dynamics equations and Section 3 surveys previous efforts to solve these equations numerically. A brief introduction to spectral interpolation is given in Section 4. The new spectral discretization approach is introduced in Section 5. Numerical results are presented in Section 6 and Section 7 draws conclusions and pinpoints future work.

2 The continuous particle dynamics equation

In this paper the continuous particle size distributions are considered functions of particle volume (v) and time (t). For simplicity we consider single component particles, but the discretization techniques can be directly generalized to multiple components. The size distribution function (number density) of a family of particles will be denoted by $n(v,t)$; the number of particles per unit volume of air with the volume between v and $v+dv$ is $n(v,t)dv$. This describes completely a population of single-component particles. Similar formulations can be given in terms of volume, surface, or mass densities [18]. However, recovering mass from a volume formulation is difficult in practice, as the densities are only approximately known and are a function of composition and size.

The aerosol population undergoes a series of physical and chemical transformations. *Growth* processes include condensation, evaporation, deposition and sublimation (of gases to/from the particle surface). The

growth of each component's volume takes place at a rate that depends on the particle's dimension and composition, $dv/dt = I(v,t)$. *Coagulation* forms new particles of volume $v+w$ from the collision of two smaller particles of volumes v and w; the collision rate $\beta_{v,w} n(v) n(w)$ is proportional to the number of available small particles; the proportionality factor (called the coagulation kernel) is usually a symmetric function, $\beta_{v,w} = \beta_{w,v}$. *Nucleation* of gases creates small particles. *Emissions* increase the number of particles of a specific composition and size, while *deposition* processes remove particles from the atmosphere. In addition, the constituents interact chemically inside each particle, changing the chemical composition (but not the number) of particles.

Under the above physical transformations the number density changes according to [6]

$$\begin{aligned} \frac{\partial n(v,t)}{\partial t} &= -\partial \left[I(v)\, n(v,t) \right] / \partial v \\ &\quad + \frac{1}{2} \int_0^v \beta_{v-w,w}\, n(v-w,t) n(w,t) dw - n(v,t) \int_0^\infty \beta_{v,w}\, n(w,t) dw \\ &\quad + S(v,t) - R(v,t)\, n(v,t) \ , \\ n(v,t=0) &= n^0(v) \ , \quad n(v=0,t) = 0 \ . \end{aligned} \tag{1}$$

The different terms in equation (1) describe, in order, the modification in the number of particles due to growth, creation of particles of volume v by coagulation, loss of volume v particles due to coagulation, increase in particle number due to nucleation, emissions and depositions (sources and sinks). The equation is subject to a specified initial condition $n^0(v)$, and to the boundary condition of no zero-volume particles.

In practice one assumes that the particle population has a nonzero minimal volume and a finite maximal volume, i.e. the dynamic equation is solved on a finite volume interval $[V_{\min}, V_{\max}]$.

$$\begin{aligned} \frac{\partial n(v,t)}{\partial t} &= -\partial \left[I(v)\, n(v,t) \right] / \partial v \\ &\quad + \frac{1}{2} \int_{V_{\min}}^{v-V_{\min}} \beta_{v-w,w}\, n(v-w,t) n(w,t) dw - n(v,t) \int_{V_{\min}}^{V_{\max}} \beta_{v,w}\, n(w,t) dw \\ &\quad + S(v,t) - R(v,t)\, n(v,t) \ , \\ n(v,t=0) &= n^0(v) \ , \quad n(V_{\min},t) = 0 \ . \end{aligned} \tag{2}$$

Particle sizes span orders of magnitude, and to reveal the particle distribution logarithmic coordinates are popular. If we denote

$$x = \log v \ , \quad y = \log w \ , \quad X_{\min} = \log V_{\min} \ , \quad X_{\max} = \log V_{\max} \ ,$$

the dynamics equation becomes

$$\begin{aligned} \frac{\partial n(x,t)}{\partial t} &= -e^{-x} \partial \left[I(x)\, n(x,t) \right] / \partial x \\ &\quad + \frac{1}{2} \int_{X_{\min}}^{\log(e^x - e^{X_{\min}})} \beta_{\log(e^x - e^y),y}\, n(\log(e^x - e^y),t) n(y,t) e^y dy - n(x,t) \int_{X_{\min}}^{X_{\max}} \beta_{x,y}\, n(y,t) e^y dw \\ &\quad + S(x,t) - R(x,t)\, n(x,t) \ , \\ n(x,0) &= n^0(x) \ , \quad n(X_{\min},t) = 0 \ . \end{aligned} \tag{3}$$

3 Previous work

Three major approaches are used to represent the size distribution of aerosols: continuous, discrete and parameterized. In this paper we focus on continuous models (i.e. continuous size distributions and the general dynamic equations in continuous form).

For computational purposes one needs to use finite-dimensional approximations of the continuous size distributions. In the *sectional approach* the size domain $v \in [0, \infty]$ is divided into size bins $v \in [V_i^{\text{low}}, V_i^{\text{high}})$. In each size bin i there are n_i particles per unit volume, all of them having the same mean volume V_i.

variations of this approach include the *full-moving* structure, the *quasi-stationary approach*, as well as the *moving-center* structure [11].

The integro-differential coagulation equation is difficult to solve accurately, due to the quadratic terms under the integral, as well as the Volterra nature of the first term. The algorithms proposed in the literature for the coagulation equation include semi-implicit solutions, finite element method, orthogonal collocation over finite elements, J-space transformations, analytical solutions [11, Section 16], [15] etc. A nice survey of several popular numerical methods for particle dynamics equations is given in Zhang et. al. [24].

Many models include different processes successively, using a time splitting scheme. This enables the use of numerical methods tuned to each subprocess but introduces hard-to-quantify splitting errors.

Jacobson [11, Section 16] proposed the semi-implicit scheme to solve the discrete coagulation equation. Kim and Seinfeld [13] extended the moving sectional method to solve the multicomponent aerosol condensation equation. A nice survey of several popular numerical methods for the growth equations is given in Zhang et. al. [24]. In UAM-AERO and SAQM-AERO [14] the boundaries of the size sections move at a rate consistent with the growth rate equation (a Godunov-type advection scheme); CIT, UAM-AIM uses the Eulerian advection scheme of Bott [3]. In GATOR [10] the mean particle size in each bin i is allowed to grow. Jacobson [9] developed a highly complex gas, aerosol, transport and radiation model (GATOR). A combination of cubic splines (coagulation) and moving finite element techniques (growth part) was used by Tsang and Hippe [23]. Meng, Dabdub and Seinfeld [16] present a size-resolved and chemically-resolved model for aerosol dynamics in a mass density formulation. Different solution of the growth equations were proposed in [2, 10, 13, 14]. Gelbard and Seinfeld [6, 7, 8] solved the coupled dynamic equations using orthogonal collocation over finite elements. Pilinis [18] derived and solved the equations that govern the time evolution of mass distribution for a multicomponent particulate system.

4 Spectral Interpolation

In this section we review some important aspects spectral interpolation. Consider the set of s Chebyshev points in the interval $[V_{\min}, V_{\max}]$ (cf. [22])

$$V_j = V_{\min} + \frac{V_{\max} - V_{\min}}{2} \left[1 - \cos\left(\frac{j-1}{s-1} \pi \right) \right] , \quad j = 1 \cdots s . \tag{4}$$

Let $f(v)$ be a function on $v \in [V_{\min}, V_{\max}]$, and $p(v)$ the unique interpolation polynomial of degree at most $s-1$ such that

$$p(V_j) = f(V_j) , \quad j = 1 \cdots s .$$

The polynomial can be expressed in terms of the Lagrange basis functions associated with the Chebyshev set of points (4); then

$$p(v) = \sum_{i=1}^{s} f(V_i)\, \mathcal{L}_i(v) , \quad \mathcal{L}_i(v) = \frac{\prod_{k \neq i} (v - V_k)}{\prod_{k \neq i} (V_i - V_k)} \text{ for all } i . \tag{5}$$

This polynomial is a very accurate approximate of f. We recall the following result from Trefethen [22, Chapter 5]; for more details the reader is invited to consult Trefethen's book.

Accuracy of spectral polynomial interpolation. If $f(v)$ is smooth enough* there exist $C_1, C_2 > 0$ (independent of s) such that the interpolation error is

$$|f(v) - p(v)| \leq C_1 e^{-C_2 s} , \text{ for all } v \in [V_{\min}, V_{\max}] . \tag{6}$$

This is called "spectral accuracy".

Moreover, at the interpolation points the derivative of p is a good approximation of the derivative of f, more exactly there exist $C_3, C_4 > 0$ (independent of s)

$$\left| \frac{\partial f}{\partial v}(V_j) - \frac{\partial p}{\partial v}(V_j) \right| \leq C_3 e^{-C_4 s} , \text{ for all } j = 1 \cdots s .$$

*Analytic in an elliptic region in the complex plane that contains the interval $[V_{\min}, V_{\max}]$.

The derivative of p at the interpolation points can be easily computed with the help of the Chebyshev differentiation matrix D_s [22, Chapter 6]

$$\begin{bmatrix} \frac{\partial p}{\partial v}(V_1) \\ \vdots \\ \frac{\partial p}{\partial v}(V_s) \end{bmatrix} = -\frac{2}{V_{\max} - V_{\min}} D_s \cdot \begin{bmatrix} p(V_1) \\ \vdots \\ p(V_s) \end{bmatrix} , \quad (D_s)_{ij} = \begin{cases} \frac{2(s-1)^2}{6} & i = j = 1 \\ 2\frac{(-1)^{i+j}}{V_i - V_j} & i = 1, 1 < j \leq s \\ -\frac{(-1)^{i+j}}{V_i - V_j} & 1 < i \neq j < s \\ -\frac{V_j}{2(1-V_j^2)} & 1 < i = j < s \\ \frac{(-1)^{i+j}}{V_i - V_j} & 1 < i \neq j < s \\ \frac{(-1)^{i+j}}{2(V_i - V_j)} & j = 1, 1 < i \leq s \\ -\frac{2(s-1)^2}{6} & i = j = s \end{cases} . \tag{7}$$

Consequently, the function derivative at the node points can be approximated with spectral accuracy by $[\partial f / \partial v(V_i)]_{1 \leq i \leq s} \approx D_s \cdot [f(V_i)]_{1 \leq i \leq s}$.

5 The discrete formulation of aerosol dynamics

We solve equation (1) by a semi-discretization in particle size (v), followed by a time integration of the resulting system of ordinary differential equations. The semi-discretization in size is done by approximating the solution with the spectral polynomial interpolant, i.e. projecting the solution and the equation on the finite-dimensional subspace spanned by Lagrange basis functions $\{\mathcal{L}_1(v), \cdots, \mathcal{L}_s(v)\}$. For simplicity we consider single-component particle populations described completely by the number density; but the ideas can be directly extended to multiple (mass or volume) distributions for multiple-component aerosols.

5.1 Discretization of the particle size distribution

From (5) one can approximate the continuous particle distribution by the spectral interpolation polynomial

$$n(v,t) = \sum_{i=1}^{s} n_i(t)\, \mathcal{L}_i(v) , \quad n_i(t) = n(V_i, t) . \tag{8}$$

The approximation is finite dimensional, with the set of time-dependent values

$$n(t) = [\, n_1(t), \cdots, n_s(t) \,]^T , \tag{9}$$

to be determined from the dynamics equation. We extend the terminology of the sectional method and and refer to $n_i(t) = n(V_i, t)$ as the number of particles in *size bin* i.

5.2 Coagulation

The theoretical coagulation equation for single-component particles is [11, Section 16]

$$\frac{\partial n(v,t)}{\partial t} = \frac{1}{2} \int_{V_{\min}}^{v - V_{\min}} \beta_{v-w,w}\, n(v-w,t) n(w,t) dw - n(v,t) \int_{V_{\min}}^{V_{\max}} \beta_{v,w}\, n(w,t) dw . \tag{10}$$

To obtain a discrete form of the coagulation equation one inserts the spectral polynomial approximation (8) into (10), and imposes the resulting equation to hold exactly at the set of node points V_j, $1 \leq j \leq s$. After some calculations one arrives at the discretized coagulation equation

$$n'(t) = \begin{bmatrix} n^T(t)\, (B^1 - C^1)\, n(t) \\ \vdots \\ n^T(t)\, (B^s - C^s)\, n(t) \end{bmatrix} , \tag{11}$$

with the matrices

$$\begin{aligned} B^j &= \left[(1/2)\int_{V_{\min}}^{v-V_{\min}} \beta_{V_j-w,w}\mathcal{L}_k(V_j-w)\mathcal{L}_m(w)dw\right]_{1\le k,m\le s} \ , \quad 1\le j\le s \ , \\ C^j &= \left[\delta_{kj}\int_{V_{\min}}^{V_{\max}} \beta_{V_j,w}\mathcal{L}_m(w)dw\right]_{1\le k,m\le s} \ , \quad 1\le j\le s. \end{aligned} \tag{12}$$

Here $\delta_{kj}=1$ for $k=j$ and 0 otherwise; consequently C matrices are very sparse. One can regard B and C as three-tensors and compactly write the discrete equation (11) as

$$n'(t) = \left[(B-C)\times n(t)\right]\cdot n(t). \tag{13}$$

A simpler formulation of the negative coagulation term is possible by a spectral interpolation the integrand $\{\beta_{v,w}\, n(w,t)\}$ in w and an integration of the resulting polynomial. The optimal weights for such integration are given by the Clenshaw-Curtis quadrature [22, Section 12]. Therefore we have

$$n(V_i,t)\int_{V_{\min}}^{V_{\max}} \beta_{V_i,w}\, n(w,t)dw \ \approx n(V_i,t)\sum_{k=1}^{s}\xi_k\beta_{V_i,V_k}\, n(V_k,t) \ ,$$

with the Clenshaw-Curtis weights $\{\xi_k\}_{1\le k\le s}$ given by the discrete cosine transform of the vector $\{\zeta_k\}_{1\le k\le s}$ with halved first and last components (cf. [5, Section 2])

$$\zeta_k = \frac{2}{1-(k-1)^2} \ \text{ for } k \text{ odd} \ , \quad \text{and } \zeta_k = 0 \ \text{ for } k \text{ even.}$$

5.3 Growth

The growth equation in number densities

$$\frac{\partial n(v,t)}{\partial t} = -\frac{\partial}{\partial v}\left[I(v)\, n(v,t)\right] \ , \quad I(v)=\frac{dv(t)}{dt} \ , \quad n(v=0,t)=0 \ , \quad n(v,t=0)=n^0(v) \ , \tag{14}$$

has the form of an advection equation, with the "flow speed" provided by the time derivative of the volume. This equation is to be solved subject to an initial distribution $n^0(v)$ and the boundary condition of no zero-sized particles [19, Section 12],

The discrete version of the growth equation is a standard application of spectral methods and is based on replacing the derivative by the spectral differentiation formula (7). This gives

$$n'(t) = -G\, n(t) \quad \text{where} \quad G = -\frac{2}{V_{\max}-V_{\min}}\, D_s\cdot \operatorname{diag}\left[I(V_1),\cdots,I(V_s)\right] \ . \tag{15}$$

To impose the homogeneous boundary condition at $v=0$ (or $v=V_{\min}$) one can strip G of its first row and first column (see [22]).

5.4 Sources and sinks

Sources (emissions, nucleation) have a simple mathematical formulation,

$$\frac{\partial n(v,t)}{\partial t} = S(v,t) \ .$$

The simplicity comes from the fact that S terms are not coupled across different volumes. The discrete evolution equations can be written for each bin as $n_i'(t)=S(V_i,t)=S_i(t)$, $1\le i\le s$. Similarly, the sinks (deposition processes)

$$\frac{\partial n(v,t)}{\partial t} = -R(v,t)\, n(v,t)$$

can be discretized as $n_i'(t) = -R(V_i,t)n_i(t) = -R_i(t)n_i(t)$. In vector notation

$$n'(t) = S(t) - R\, n(t) \ , \quad R = \operatorname{diag}\left\{\, R_1(t),\cdots,R_s(t)\,\right\} \ . \tag{16}$$

5.5 Simultaneous discretization of the dynamic equations

A coupled solution of coagulation, growth, nucleation, emissions and deposition is of interest; it will, for example, better capture the competition between nucleation of new particles and condensation on existing particles for gas-to-particle conversion [24].

For single component particles combining (11), (15) and (16) gives the semi-discrete aerosol dynamics equation

$$n'(t) = \underbrace{-G\,n(t)}_{\text{growth}} + \underbrace{[(B-C)\times n(t)]\;n(t)}_{\text{coagulation}} + \underbrace{S(t)}_{\text{nucl.+em}} \underbrace{-R\,n(t)}_{\text{dep.}} \;. \tag{17}$$

This is a system of s coupled ordinary differential equations. The discrete initial conditions are

$$n(0) = \left[\; n^0(V_1)\cdots n^0(V_s)\;\right]^T \;. \tag{18}$$

5.6 Time integration

The system (17)-(18) can be solved by any appropriate time-stepping method. The system has a particular form: the growth term is linear, while the coagulation term is bilinear. The Jacobian of the coagulation term can be expressed as

$$J^{\text{coag}}(n) = \begin{bmatrix} n^T\{(B^1-C^1)+(B^1-C^1)^T\} \\ \vdots \\ n^T\{(B^s-C^s)+(B^s-C^s)^T\} \end{bmatrix} \;.$$

Depending on stability restrictions any explicit or implicit method can be applied to solve (17)-(18).

Particularly attractive are linearized versions of the implicit numerical methods which preserve stability yet avoid iterative solutions. The following method combines a linearized backward Euler scheme for coagulation with Crank-Nicholson for growth and sources/sinks to achieve second order time accuracy:

$$\left(I - \frac{\Delta t}{2}J^{\text{coag}}(n^k) - \frac{\Delta t}{2}(G+R)\right) n^{k+1} = \left(I + \frac{\Delta t}{2}(G+R)\right) n^k + \frac{\Delta t}{2}\left(S(t^{k+1}) + S(t^k)\right) \;. \tag{19}$$

As usual n^k, n^{k+1} denote the numerical approximations of $n(t^k)$ and $n(t^{k+1})$, with the time moments related by $t^{k+1} = t^k + \Delta t$. G and R are evaluated at t^k.

5.7 Multiple chemical components

Complex models treat particles composed of multiple chemical constituents. Let $v_q(v,t)$, $q = 1,\cdots,m$ be the volume of the q-th chemical component in particles of volume v; the multi-component aerosol population is described by the individual volume densities of each constituent $\mathcal{V}^q(v,t) = v_q(v,t)\,n(v,t)$; the total volume of component q (per unit volume of air) contained in all particles having individual volumes between v and $v+dv$ is $\mathcal{V}^q(v,t)dv$. Under these transformations the volume densities of each constituent $\mathcal{V}^q(v,t)$, $q = 1,\cdots,m$ change according to [6, 18]

$$\begin{array}{lll} \partial\mathcal{V}^q(v,t)/\partial t & = & \\ \text{(growth)} & & -\,\partial\left[\mathcal{V}^q(v,t)\,\sum_{k=1}^m I_k(v,t)\right]/\partial v + \mathcal{V}(v,t)I_q(v,t)/v \\ \text{(coagulation)} & & +\,\int_0^v \frac{\beta_{v-w,w}}{w}\,\mathrm{V_q}(v-w,t)\mathcal{V}(w,t)dw - \mathrm{V_q}(v,t)\int_0^\infty \frac{\beta_{v,w}}{w}\,\mathcal{V}(w,t)dw \\ \text{(sources)} & & +\,S_q(v,t) \\ \text{(deposition)} & & -\,R_q(v,t)\,V_q(v,t) \\ \text{(chemistry)} & & +\,K(\mathcal{V}_1,\cdots,\mathcal{V}_m,t)\;, \qquad\qquad q = 1,\cdots,m\;, \end{array} \tag{20}$$

where $\mathcal{V}(v,t) = \sum_{q=1}^m \mathcal{V}^q(v,t)$ is the total volume distribution; the m integro-differential equations are coupled through $\mathcal{V}(v,t)$ and $K(\mathcal{V}_1,\cdots,\mathcal{V}_m,t)$. The system (20) is subject to the initial and boundary conditions

$$\mathcal{V}^q(v,t=0) = (\mathcal{V}^q)^0(v)\;, \quad \mathcal{V}^q(v=0,t) = 0\;, \quad q = 1,\cdots,m\;. \tag{21}$$

The equations (20)-(21) can be discretized in size using the same approach. For each component volume one has

$$\mathcal{V}^q(v,t) = \sum_{i=1}^{s} \mathcal{V}_i^q(t)\, \mathcal{L}_i(v) \ , \quad \mathcal{V}_i^q(t) = \mathcal{V}^q(V_i,t) \ , \quad q = 1, \cdots, m \ , \tag{22}$$

and the semidiscrete system reads

$$\begin{aligned} \frac{d}{dt}\mathcal{V}^q(t) \quad = \quad & \underbrace{-G\,\mathcal{V}^q(t) + \mathrm{diag}_i\left(\frac{I_q(V_i)}{V_i}\right)\sum_{k=1}^{m}\mathcal{V}^k(t)}_{\text{growth}} \\ & \underbrace{+\left[B \times \mathcal{V}^q(t)\right]\mathcal{V}^q(t) - \left[C \times \sum_{k=1}^{m}\mathcal{V}^k(t)\right]\mathcal{V}^q(t)}_{\text{coagulation}} \\ & + \underbrace{S(t)}_{\text{nucl.+em}} \ \underbrace{- R_q\,\mathcal{V}^q(t)}_{\text{dep.}} + \underbrace{K(\mathcal{V}^1, \cdots, \mathcal{V}^m, t)}_{\text{chem.}} \ , \quad q = 1, \cdots, m \ . \end{aligned}$$

The matrix G and the tensors B and C are redefined according to (20). Note that the same G, B, C are used for all q's, which makes the method efficient.

6 Numerical experiments

Test problem. For the numerical experiments we first consider the test problem from [7], which admits an analytical solution. Let N_t be the total initial number of particles and V_m the mean initial volume. The initial number distribution is exponential, the coagulation rate is constant, and the growth rate is linear with the volume:

$$N_\mathrm{t}(v) = (N_\mathrm{t}/V_\mathrm{m})\, e^{-v/V_\mathrm{m}} \ , \quad \beta(v,w) = \beta_0 \ , \quad I(v) = \sigma\, v \ .$$

This test problem admits an analytical solution, which is given in [7]

$$n^A(v,t) = \frac{4N_\mathrm{t}}{V_\mathrm{m}(N_\mathrm{t}\beta_o t + 2)^2} \cdot \exp\left(\frac{-2v\exp(\sigma_o t)}{V_\mathrm{m}(N_\mathrm{t}\beta_o t + 2)} - \sigma_o t\right) \ .$$

We solve the dynamics equation for $\beta_o = 6.017 \times 10^{-10}$ cm^{3}sec^{-1}particles^{-1}, $\sigma_o = 0.03$ hour^{-1}, $N_\mathrm{t} = 10^4$ particles, $V_\mathrm{m} = 0.03\ \mu$m^3. The value of σ_o is chosen such that coagulation and growth have effects of comparable magnitude.

The equation was solved on the time interval $[\, t_0 = 0,\ t_\mathrm{final} = 6 \text{ hours}\,]$, with a small time step, $\Delta t =$ 1 second. The volume interval $[\, V_\mathrm{min} = \pi/6 \times 10^{-9}\ \mu\mathrm{m}^3,\ V_\mathrm{max} = \pi/6\ \mu\mathrm{m}^3\,]$ corresponds to a particle diameter range $[\, D_\mathrm{min} = 10^{-3}\ \mu$m, $D_\mathrm{max} = 1\ \mu\mathrm{m}\,]$.

The numerical error is measured against the analytical solution by the root-mean-square (RMS) error norm

$$\|E\| = \sqrt{\frac{1}{s}\sum_{i=1}^{s}\left(\frac{n\left(V_i, t_\mathrm{final}\right) - n^A\left(V_i, t_\mathrm{final}\right)}{\max(n^A\left(V_i, t_\mathrm{final}\right), th)}\right)} \ . \tag{23}$$

The threshold $th = 100$ particles makes the error indicator to ignore part of the small long tail of the exponential distribution. The use of a finite volume interval for the given problem introduces errors in the coagulation right-hand-side of the order of 10^{-8}. The best accuracy we can hope for is consequently of this magnitude regardless of how many size bins we use.

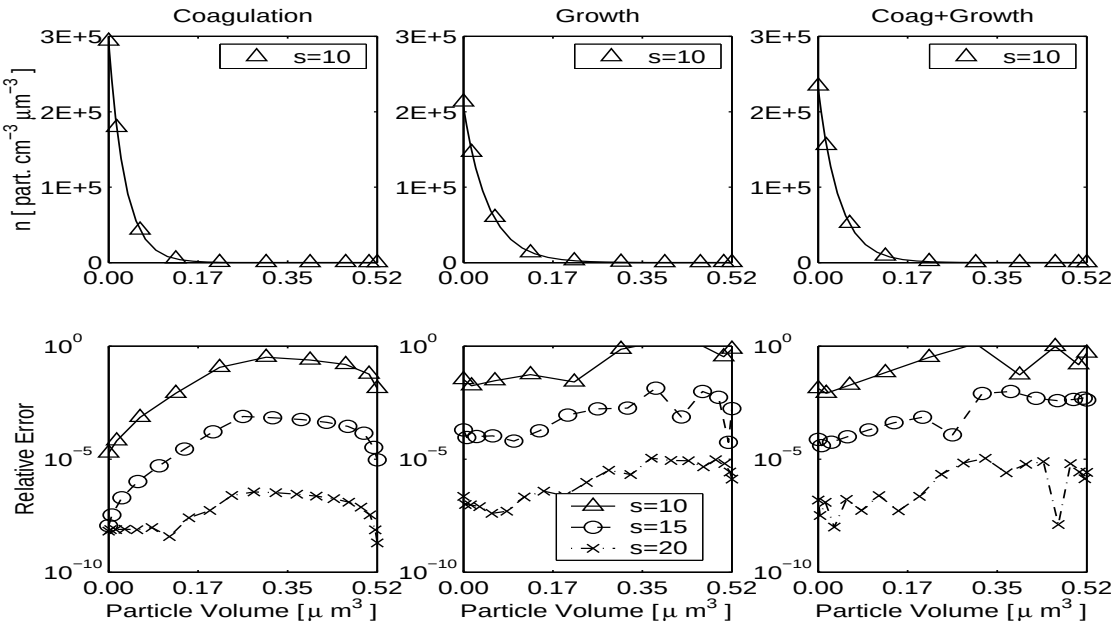

Figure 1: Experiment I (linear coordinates). The exact solution at $t_{\text{final}} = 6$ hours for coagulation only, growth only, and coagulation-growth problems and the distribution of relative errors for different numbers of grid points.

Experiment I - Linear. In this experiment we solve the test problem (2) in the linear volume coordinate. We consider separately the coagulation-only and growth-only problems in addition to coagulation and growth.

Figure 1 shows the exact solution, the numerical solution with $s = 10$ as well as the error distribution with volume. The numerical solutions for $s = 10$ reproduce quite well the exact solutions for all tests. For larger numbers of bins the errors decrease rapidly.

Figure 2 plots the error norm of the solution at the end of the simulation versus the number of bins; the errors decrease rapidly. The error plots are nearly straight lines and the axes are logarithmic in $\|E\|$ and linear in s; this is in agreement with (6) and illustrates the spectral accuracy of the method.

Experiment II - Logarithmic. Now we solve the test equation in the logarithmic formulation (3) . The approach is similar in that we use spectral interpolation in the $x = \log v$ variable. The results are shown in Figure 3. The solution to coagulation problem is fairly accurate for small volumes, but the error increases

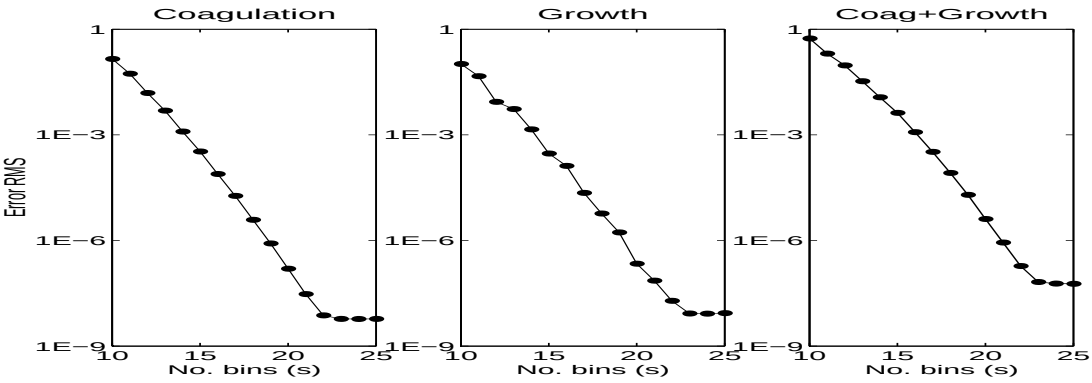

Figure 2: Experiment I (linear coordinates). RMS Error norms for the solution at $t_{\text{final}} = 6$ hours for coagulation only, growth only, and coagulation-growth problems.

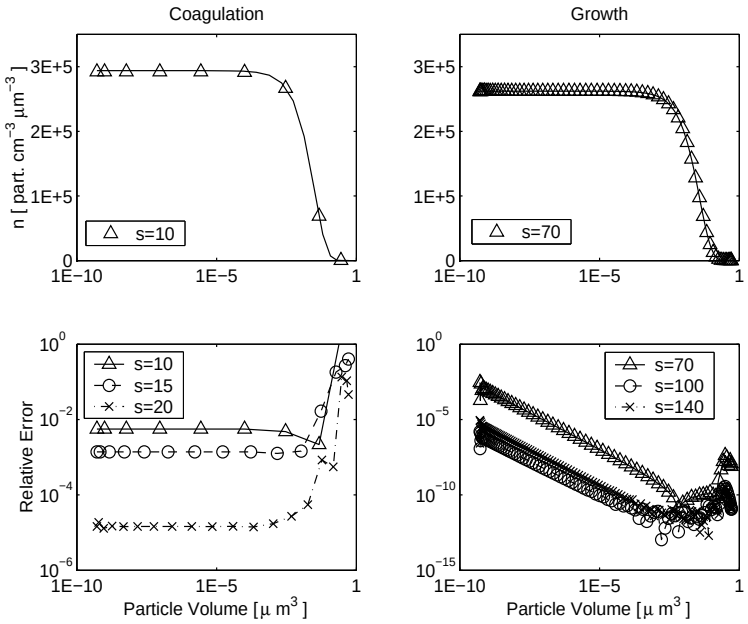

Figure 3: Experiment II (logarithmic coordinates). The exact solution at $t_{\text{final}} = 6$ hours for coagulation only, and growth only problems and the distribution of relative errors for different numbers of grid points.

toward the tail of the exponential distribution. The errors decrease with increasing s but they do not display spectral accuracy.

The solution to the growth problem is rather disappointing: one needs at least 70 gridpoints to reproduce the solution at small volumes (for smaller s the solution oscillates at small particle volumes). Clearly the growth problem in logarithmic coordinates is ill-scaled.

Experiment III - Logarithmic. We now consider a second test problem that is posed in naturally logarithmic coordinates. Here $\beta_o = 1.083 \times 10^{-3}$ cm^3 hour^{-1} particles^{-1}, $I(v) = 0.02$ μm^{3}hour^{-1} = const, and $N_{\text{t}} = 10^4$ particles. The volume interval is $V_{\min} = 10^{-3}$ μm^3, $V_{\max} = 1$ μm^3, the time interval [$t_0 = 0$, $t_{\text{final}} = 6$ hours], and the time step $\Delta t = 1$ second.

The initial concentration is a cosine hill in logarithmic coordinates

$$n_0(v) = \begin{cases} \frac{N_{\text{t}}}{2} \cdot \left[1 - \cos\left(2\pi \frac{\log v - x_{\min}}{x_{\max} - x_{\min}}\right)\right] , & \log V_{\min} < x_{\min} < \log v < x_{\max} < \log V_{\max} . \\ 0 , & \log v \le x_{\min} \text{ or } \log v \ge x_{\max} . \end{cases}$$

The reference solution was obtained using the standard numerical method for coagulation [11] on the uniform grid $V_i = i \cdot \Delta v$, $\Delta v = 10^{-3}$ μm^3, such that $V_1 = V_{\min}$ and $V_{1000} = V_{\max}$. The reference growth-coagulation solution is obtained by translating the reference coagulation solution 20 gridpoints to the right.

Figure 4 shows the results. A meaningful solution for coagulation can be obtained with as few as 7 bins. For growth one needs at least 50 points to obtain a good numerical solution. Other experiments (not reported here) showed that 20 points are sufficient to solve growth in linear coordinates (although part of the profile is lost due to insufficient resolution.

To solve the coagulation-growth problem the obvious approach is to increase the number of bins to 50, such that each subproblem is treated correctly; the cost of building 50-dimensional tensors for coagulation is however significant.

In order to avoid these extra costs we propose the following approach, based on different grids for coagulation and for growth. Let $\{x_i\}$, $1 \le i \le s$ and $\{x'_j\}$, $1 \le j \le s'$ be two sets of Chebyshev points on $[V_{\min}, V_{\max}]$ (x and y are two grids with different number of points). If the function N is represented on grid

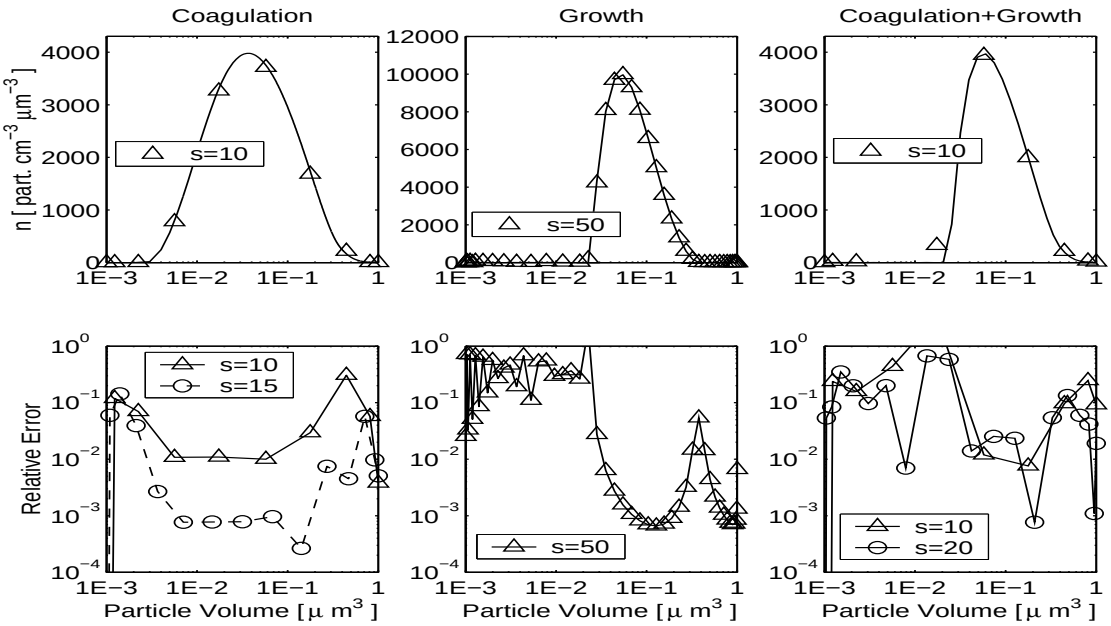

Figure 4: Experiment III (logarithmic coordinates). The exact solution at $t_{\text{final}} = 1$ hours for coagulation, growth, and coupled problems and the distribution of relative errors for different numbers of grid points.

x as $[N_1, \cdots, N_s]^T$ then a representation on the grid y is given by spectral interpolation:

$$\begin{bmatrix} N_1' \\ \vdots \\ N_{s'}' \end{bmatrix} = \left[\mathcal{L}_i(x_j') \right]^T_{1\le i\le s, 1\le j\le s'} \cdot \begin{bmatrix} N_1 \\ \vdots \\ N_s \end{bmatrix} = T^{x,x'} \cdot \begin{bmatrix} N_1 \\ \vdots \\ N_s \end{bmatrix} ,$$

where $\mathcal{L}_i$ are Lagrange basis polynomials associated with the points $\{x_i\}$.

This allows us to use a finer grid for growth and a coarser grid for coagulation (say with 50 and 10 gridpoints respectively). The method can be formulated on the fine grid as

$$\left(I - \frac{\Delta t}{2} T^{\text{up}} \cdot J^{\text{coag}}\left(T^{\text{down}} n^k\right) \cdot T^{\text{down}} - \frac{\Delta t}{2} G \right) n^{k+1} = \left(I + \frac{\Delta t}{2} G \right) n^k \ . \tag{24}$$

where T^{down} and T^{up} are the transformation matrices from fine to coarse and from coarse to fine (it is easy to see that coagulation is solved on the coarse grid).

The results are displayed in Figure 4 (rightmost column). The results with 50 gridpoints for growth and 10 gridpoints for coagulation reproduce the reference solution quite well. The error norms – as measured by (23) – do not decrease below 10^{-3}, a value consistent with the growth errors on 50 points.

7 Conclusions

Aerosols are becoming an important topic in air pollution modeling. For a correct representation of particles in the atmosphere one needs to accurately solve for the size distribution of particle populations.

In this work we develop a discretization method for aerosol dynamics equation based on approximating the solution by a spectral polynomial interpolant. The resulting semidiscrete system is bilinear and is solved by a second order order linearly-implicit time stepping method.

The present formulation of the discretization method is based on number densities and single-component particles. The same ideas apply directly to volume, surface and mass densities, as well as to multiple densities that model multiple-component aerosols.

To illustrate the power of the method we employed two test problems: one with analytical solution in the infinite volume range $v \in [0, \infty]$; and a second one with the solution "living" in a finite volume interval and formulated in logarithmic coordinates.

In the standard formulation (linear coordinates) the numerical solution displays spectral accuracy – the errors decrease exponentially fast as the number of bins is increased. In logarithmic coordinates (preferred by environmental modelers) good solutions can be obtained for the coagulation equation; but the growth problem is ill-scaled and can be solved accurately only by increasing the number of bins. A mixed solution is proposed to solve growth on a fine grid and coagulation on a coarse grid. Spectral accuracy is not observed in logarithmic coordinates, although the numerical solutions reproduce quite well the reference solutions.

Future work will focus on testing the spectral discretization method on multiple component particles and on coupled aerosol dynamics and chemistry models.

Acknowledgments

This work was supported by NSF CAREER award ACI-0093139.

References

[1] K.E. Atkinson. *The Numerical Solution of Integral Equations of the Second Kind.* Cambridge University Press, 1997.

[2] F.S. Binkowski and U. Shankar. The regional particulate matter model: 1: model description and preliminary results. *Journal of Geophysical research*, 100:26,191–26,209, 1995.

[3] A. Bott. A positive definite advection scheme obtained by nonlinear renormalization of the advection fluxes. *Monthly Weather Review*, 117:1006–1115, 1989.

[4] V. Ramanathan, P.J. Crutzen, M.O. Andreae, J. Coakley, R. Dickerson, J. Heintzenberg, A. Heymsfield, J.T. Kiehl, D. Kley, T.N. Krishnamurti, J. Kuettner, J. Lelieveld, S.C. Liu, A.P. Mitra, J. Prospero, R. Sadourny, A.F. Tuck, and F.P.J. Valero. Indoex white paper. Indian Ocean Experiment, http://www-indoex.ucsd.edu/publications/white_paper, 1998.

[5] L.M. Delves and J.L. Mohamed. *Computational methods for integral equations.* Cambridge University Press, 1985.

[6] F.M. Gelbard and J.H. Seinfeld. Coagulation and growth of a multicomponent aerosol. *Journal of Colloid and Interface Science*, 63(3):472–479, 1978.

[7] F.M. Gelbard and J.H. Seinfeld. Numerical solution of the dynamic equation for particulate systems. *Journal of Computational Physics*, 28:357–375, 1978.

[8] F.M. Gelbard and J.H. Seinfeld. Simulation of multicomponent aerosol dynamics. *Journal of Colloid and Interface Science*, 78(2):485–501, 1980.

[9] M.Z. Jacobson. Development and application of a new air pollution modeling system - II. Aerosol module structure and design. *Atmospheric Environment*, 31(2):131–144, 1997.

[10] M.Z. Jacobson. Numerical techniques to solve condensational and dissolutional growth equations when growth is coupled to reversible reactions. *Aerosol Science and Technology*, 27:491–498, 1997.

[11] M.Z. Jacobson. *Fundamentals of atmospheric modeling.* Cambridge University Press, 1999.

[12] C. Johnson. *Numerical Solution of Partial Differential Equations by the Finite Element Method.* Cambridge University Press, 1987.

[13] Y.P. Kim and J.H. Seinfeld. Simulation of multicomponent aerosol condensation by the moving sectional method. *Journal of Colloid and Interface Science*, 135(1):185–199, 1990.

[14] F.W. Lurmann, A.S. Wexler, S.N. Pandis, S. Musara, N. Kumar, and J.H. Seinfeld. Modeling urban and regional aerosols - ii. application to California's south coast air basin. *Atmospheric Environment*, 31:2695–2715, 1997.

[15] A.A. Lushnikov. Evolution of coagulating systems iii. coagulating mixtures. *Journal of Colloid and Interface Science*, 54(1):94–101, 1976.

[16] Z. Meng, D. Dabdub, and J.H. Seinfeld. Size-resolved and chemically resolved model of atmospheric aerosol dynamics. *Journal of Geophysical Research*, 103(D3):3419–3435, 1998.

[17] M. Phadnis and G.R. Carmichael. Transport and distribution of primary and secondary non-methane hydrocarbons in east Asia under continental outflow conditions. *J. Geophys. Res.*, in press, 1999.

[18] C. Pilinis. Derivation and numerical solution of the species mass distribution equation for multicomponent particulate systems. *Atmospheric Environment*, 24A(7):1923–1928, 1990.

[19] J.H. Seinfeld and S.N. Pandis. *Atmospheric chemistry and physics. From air pollution to climate change.* John Wiley & Sons, Inc., 1997.

[20] C.H. Song and G.R. Carmichael. Partitioning of hno3 modulated by alkaline aerosol particles. *J. Geophys. Res.*, in review, 1999.

[21] C.H. Song, G.R. Carmichael, and S.Y. Cho. An alternative way to couple kinetic (non-equilibrium/condensation/evaporation process with thermodynamic equilibrium relationships. *Atmospheric Environment*, to be submitted, 1999.

[22] L.N. Trefethen. Spectral methods in Matlab. SIAM Software, Environments, Tools Series, 2000.

[23] H. Tsang and J.M. Hippe. Asymptotic behavior of aerosol growth in the free molecule regime. *Aerosol Science and Technology*, 8:265–278, 1988.

[24] Y. Zhang, J.H. Seinfeld, M.Z. Jacobson, and F.S. Binkowski. Simulation of aerosol dynamics: a comparative review of algorithms used in air quality models. *submitted to AS&T*, 1999.